CORA

Cork Open Research Archive
Cartlann Taighde Oscailte Chorcaí

| Title | Multichannel ultrasonic data communications in air using range-dependent modulation schemes |
|---|---|
| Author(s) | Jiang, Wentao; Wright, William M. D. |
| Publication date | 2016-01 |
| Original citation | Jiang, W. and Wright, W. M. D. (2016) 'Multichannel ultrasonic data communications in air using range-dependent modulation schemes', IEEE Transactions on Ultrasonics, Ferroelectrics, and Frequency Control, 63(1), pp. 147-155. doi:10.1109/TUFFC.2015.2498479 |
| Type of publication | Article (peer-reviewed) |
| Link to publisher's version | http://dx.doi.org/10.1109/TUFFC.2015.2498479 Access to the full text of the published version may require a subscription. |
| Rights | © 2016, IEEE. Personal use of this material is permitted. Permission from IEEE must be obtained for all other uses, in any current or future media, including reprinting/republishing this material for advertising or promotional purposes, creating new collective works, for resale or redistribution to servers or lists, or reuse of any copyrighted component of this work in other works. http://www.ieee.org/publications_standards/publications/rights/copyright policy.html |
| Item downloaded from | http://hdl.handle.net/10468/4462 |

University College Cork, Ireland
Coláiste na hOllscoile Corcaigh

# Multi-channel ultrasonic data communications in air using range-dependent modulation schemes

Wentao Jiang, *Student Member, IEEE* and William M. D. Wright, *Senior Member, IEEE*
School of Engineering - Electrical and Electronic Engineering
University College Cork, Cork, Ireland
Email: w.jiang@umail.ucc.ie, bill.wright@ucc.ie

*Abstract*—There are several well-developed technologies of wireless communication such as radio frequency (RF) and infrared (IR), but ultrasonic methods can be a good alternative in some situations. A multi-channel airborne ultrasonic data communication system is described in this paper. On-Off Keying (OOK) and binary phase-shift keying (BPSK) modulation schemes were implemented successfully in the system by using a pair of commercially available capacitive ultrasonic transducers in a relatively low multi-path indoor laboratory environment. Six channels were used from 50 kHz to 110 kHz with a channel spacing of 12 kHz, allowing multiple 8-bit data packets to be transmitted simultaneously. The system data transfer rate achieved was up to 60 kb/s, and ultrasonic wireless synchronization was implemented, instead of using a hard-wired link. A model developed in the work could accurately predict ultrasonic signals through the air channels. Signal root mean square (RMS) values and system bit error rates (BER) were analysed over different distances. Error-free decoding was achieved over ranges up to 5 m using a multi-channel OOK modulation scheme. To obtain the highest data transfer rate and the longest error-free transmission distance, a range-dependent multi-channel scheme with variable data rates, channel frequencies and different modulation schemes, was also studied in the work. Within 2 m, error-free transmission was achieved using 5-channel OOK with a data rate of 63 kb/s. Between 2 and 5 m, 6-channel OOK with 60 kb/s data transfer rate was error-free. Beyond 5 m, the error-free transmission range could be extended up to 10 m using 3-channel BPSK with a reduced data rate of 30 kb/s. The situation when two transducers were misaligned using 3-channel OOK and BPSK schemes was also investigated in the work. It was concluded that error-free transmission could still be achieved with a lateral displacement of less than 7% and oblique angles of less than 7°, and 3-channel BPSK proved to be more robust than 3-channel OOK with transducer misalignment.

*Keywords— Multi-channel Communication; Capacitive Ultrasonic Transducer; Air-coupled Ultrasound; OOK and BPSK Modulation; Wireless Synchronization; Bit Error Rate*

## I. INTRODUCTION

SHORT-RANGE indoor wireless communication is now ubiquitous. Due to its flexibility, convenience and remote control without wiring and cabling, different wireless technologies have emerged. Most applications used today are based on radio frequency (RF) and infrared (IR) systems [1], [2], but very few use ultrasonic waves as a means of transmitting signals. RF signals can interfere with other electronic equipment

such as aircraft instrumentation and medical electronics. Moreover, due to the penetrative nature of RF communications, the signal is very easy to intercept remotely [3]. IR technology [2], [4] can provide privacy because of its directivity, but a line-of-sight (LOS) connection is necessary. Its output power is also limited due to eye safety regulations [2]. Unlike the RF band, ultrasonic transmissions are unregulated and interference free to most electronic devices. In addition, ultrasonic signals in air are difficult to intercept through solid barriers as ultrasonic waves are not as penetrating as radio waves. So it may prove beneficial in certain circumstances to establish a secure indoor communication link using ultrasonic technology, as an ideal alternative to both RF and IR based solutions.

Wireless air-coupled ultrasonic communication applications have been proposed by several authors. For instance, an ultrasonic communication system including an omnidirectional transducer and a cordless earpiece with an ultrasonic microphone has been designed [5]. Similar work looked at the invention of a hands-free ultrasonic telephone with a designed bit rate of 1-10 kb/s at a frequency band between 200 kHz to 400 kHz [6]. An indoor data communications system based on ultrasound was also developed as the core of an indoor positioning system with a very low data rate of 100 b/s [7]. Later work investigated several different modulation schemes including On-Off Keying (OOK), binary frequency shift keying (BFSK) and binary phase shift keying (BPSK) in an air-coupled ultrasonic communication system [8]. However, this system suffered from high bit error rates of 50% at 2.38 m for OOK and 10% at 2.8 m for BPSK. Another later study implemented quadrature modulation using a pair of prototype micromachined capacitive ultrasonic transducers and achieved a bit rate of 200 kb/s over a distance of 1.2 m in air [9]. In this research, synchronization was achieved by establishing a hardwired link between the transmitter side and the receiver side which significantly simplified the demodulation. Previous preliminary studies by the authors investigated a multi-channel OOK scheme at a data rate of 60 kb/s over ranges within 1.2 m, however, there were significant bit errors at all channels over all ranges [10]. In this work, no extra filtering technique was used to eliminate spectral leakage and reduce channel width. It is noted that none of these previous works have achieved error-free long range transmissions for practical use, and most used hardwired synchronisation. It should also be noted that, for multi-carrier wireless transmissions, other studies have successfully implemented systems where data could be sent

ultrasonically through air or solid materials but with relatively low data rates [11], [12]. In [11], a modulation scheme with only two carriers with a very low data rate of 5.3 kb/s was proposed for an ultrasonic localization system, while in [12] a multi-channel FSK scheme was implemented for communications through metal with a poor bandwidth efficiency of 0.36 b/s/Hz.

The objective of this work is to achieve a practical ultrasonic communication system with a range-dependent modulation scheme to achieve the highest data rate and longest error-free transmission range possible using a pair of commercially available air-coupled capacitive transducers with wireless ultrasonic synchronization, and create a simulation model that can precisely predict ultrasonic signals through the air channel. It should be noted that the work was performed in a relatively low multi-path indoor environment and with negligible air turbulence to influence the data transmission. The modulation schemes and pulse shaping methods used are introduced in the next section, followed by the experimental set-up in section III. The over-all system as well as the background noise are also characterised in this section. In section IV, the ultrasonic signal was simulated and its decoding is described. Section V presents the experimental results including root mean square (RMS) values of the experimental signal compared with theoretical predictions and bit error rate (BER) tests respectively. In Sections VI and VII, ultrasonic transmission in air using the range-dependent modulation schemes with variable data transfer rates and in misaligned conditions are presented respectively. Section VIII gives the conclusions of this work.

## II. Modulation schemes and pulse shaping

In wireless communications, baseband signals are modulated into carrier waves that can be physically transmitted to match the characteristics of the channel [13]. One of the most popular digital modulation schemes is amplitude shift keying (ASK). The source generates carrier signals with large amplitude when a bit "1" occurs, and small amplitude when bit a "0" occurs. A simplified version is OOK, in which the source sends no signal when a bit "0" occurs [14]. OOK was shown to be more power efficient and more accurate than an ASK scheme in an airborne ultrasonic communication system in previous work [15]. Another modulation scheme used is BPSK. It uses two opposite signal phases (0 and 180 degrees) to convey information bits "1"s and "0"s [14]. It has been shown in previous work [8] that BPSK was the most robust modulation scheme in air-coupled ultrasonic communication with a low BER performance compared to OOK and BFSK. BFSK is not studied in this work due to its poor bandwidth efficiency. Therefore, both the OOK and BPSK techniques are investigated in this work, for the evaluation of system performance using the available ultrasonic band. To further improve bandwidth efficiency, multiple parallel communication channels over different frequencies are combined and broadcast over the same transmission path.

For a binary message, one of the states is usually zero. Therefore, an OOK modulated waveform consists of many bursts of a sinusoid. There are sharp discontinuities at the transition points in any OOK signal which result in unnecessary spectral leakage. The same problem occurs with BPSK modulated signals due to the sudden phase changes between "1"s and "0"s. In a multi-channel system, on the other hand, limiting the power of every modulated carrier to just the carrier bandwidth is important as the transmission power is reduced when the signal has a more concentrated frequency range. Apart from that, limiting a channel to a certain frequency band eliminates adjacent channel interference. Thus, in the pursuit of using the existing limited bandwidth most efficiently, introducing pulse shaping techniques is necessary to improve the signal transmission. This can be done by applying a low-pass filter, and one of the most commonly used filters is a raised cosine filter. Its transfer function $H_{RC}$ in the frequency domain is given by [16]

$$H_{RC}(f) = \begin{cases} 1, & |f| \leq \frac{1-\alpha}{2T_s} \\ cos^2(\frac{\pi T_s}{2\alpha}(|f| - \frac{1-\alpha}{2T_s})), & \frac{1-\alpha}{2T_s} \leq |f| \leq \frac{1+\alpha}{2T_s} \\ 0, & otherwise \end{cases}$$

(1)

and characterised by two factors, $\alpha$, the roll-off factor, ranging from 0 to 1, and $T_s$, the reciprocal of the symbol-rate. A value of $\alpha = 0$ gives the narrowest bandwidth, but the slowest rate of decay in the time domain. The effective bandwidth increases with increasing $\alpha$. Best choices of roll-off factors for different modulation schemes can significantly reduce inter-channel interference, thus enabling more sub-carrier channels to be fitted into limited transmission bandwidth.

## III. Apparatus and experiment

The multi-channel OOK and BPSK modulation schemes were investigated experimentally in a prototype ultrasonic communication system using a pair of Senscomp series 600 transducers [17] as shown in Fig. 1. The transducers are specially designed for operation in air at an ultrasonic frequency of 50 kHz with a beam angle of 15° at -6 dB. These devices are composed of a metallised Kapton membrane and a rigid contoured metal backplate with an aperture size of 38.4 mm. The data to be transmitted were encoded and modulated in MATLAB (MathWorks) before sending to a TTi TGA12102 arbitrary waveform generator via a GPIB interface. The signal was then amplified by a factor of 50 by a Falco WMA-300 high voltage amplifier, and combined with a bias voltage of +200 V generated by a Delta Elektronika SM3004-D power supply. The receiver was connected to a Cooknell CA6/C charge amplifier powered by a Cooknell SU2/C power supply unit, and followed by a high performance PicoScope 6403A PC oscilloscope. After that, the signal was sent to another PC through a USB interface for signal processing.

The overall system impulse response and frequency response over a typical range of 2 m are shown in Fig. 2(a) and 2(b) respectively. The received impulse was measured by sending a pulse signal generated by a Panametrics 500PR pulser from the transmitter transducer to the receiver transducer through an air gap. As can be seen in Fig. 2(b), the spectrum peaks at about 50 kHz as expected, and it indicates
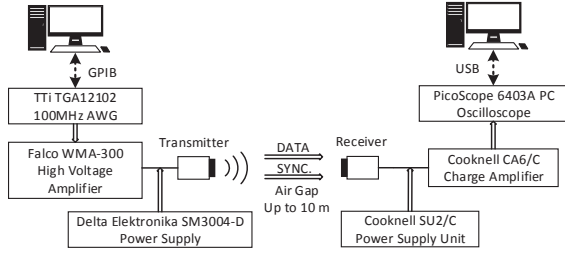
Fig. 1: Schematic diagram of the experimental arrangement showing the ultrasonic synchronization link.
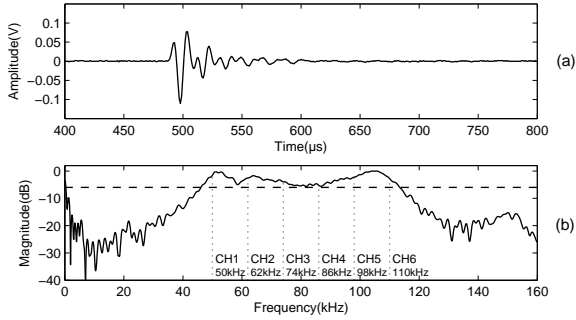


Fig. 2: System characteristics over 2 m: (a) impulse response and (b) frequency response showing the channel frequencies used.

using data channels at frequencies from 46 kHz to 112 kHz is appropriate in terms of 6-dB bandwidth which is about 66 kHz. However, in many industrial applications, acoustic noise is observed at frequencies up to 40 kHz [4]. Thus, higher operating frequencies are preferred. Initially, this work used six frequency channels from 50 kHz to 110 kHz with a channel spacing of 12 kHz. The recorded impulse peak-to-peak signal amplitude was approximately 187 mV and the background noise level was about 3 mV giving a signal-to-noise ratio (SNR) of 35.8 dB at this range.

## IV. NUMERICAL SIMULATION

A simulation of multi-channel modulation schemes was undertaken, using MATLAB, to look at the performance of a signal transmitted through each ultrasonic channel, to evaluate the demodulation process and to predict the system response at different frequencies and ranges.

### A. Ultrasonic attenuation

Ultrasonic absorption in air was considered when simulating. The atmospheric absorption factor $\alpha$ is proportional to propagation distance and can be expressed as [18]:

$$\alpha = f^2 \left[ 1.59 \times 10^{-10} \left( \frac{P_0}{P} \right) \left( \frac{T}{T_0} \right)^{\frac{1}{2}} + \right.$$

$$\left. 0.111 \left( \frac{T}{T_0} \right)^{-\frac{5}{2}} \frac{e^{\frac{-2239.1}{T}}}{f_{r,O} + \frac{f^2}{f_{r,O}}} + 0.929 \frac{e^{\frac{-3352}{T}}}{f_{r,N} + \frac{f^2}{f_{r,N}}} \right], \quad (2)$$

in dB/m. Here, $P_0$ is standard atmospheric pressure (101.325 kPa), and $P$ is the measured pressure. $T_0$ and $T$

are standard atmospheric temperature (293.15 K) and the measured temperature (in K) respectively. $f$ represents sound frequency. The terms $f_{r,O}$ and $f_{r,N}$ are respectively the scaled relaxation frequencies for oxygen and nitrogen in Hertz whose values depend on the relative humidity, measured temperature and atmospheric pressure [19].

Due to ultrasonic diffraction, it is also necessary to consider beam spread over different transmission distances. Depending on the range, different amounts of the transmitted energy will be intercepted by the receiver. Beam spread for a circular transducer is a function of the transducer diameter and the wavelength in the medium through which the sound is travelling [20]. The beam spread angle $\theta$ is given by:

$$\sin(\theta/2) = 1.22\lambda/D, \quad (3)$$

where $\lambda$ is the ultrasonic wavelength and $D$ is the aperture of the ultrasonic transmitter. This equation for beam spread is only valid for $\lambda \ll D$ and thus becomes increasingly inaccurate with low frequency signals using small transducer sources [21]. It is noted that only in the Fraunhofer region, or far field, the maximum sound pressure is found along the centreline of the transducer [20]. For Senscomp transducers, the near-field lengths of 50 kHz and 110 kHz signals at $20°C$ are 52 mm and 117 mm respectively. The transmission range was thus set beyond 117 mm in simulation. According to (3), in the far field, ultrasonic beams are more diverged when transmitting a low frequency signal. Consequently, a receiver with the same diameter as the transmitter receives less energy per unit area from a low frequency signal than from a high frequency signal at the same range before considering ultrasonic attenuation in air. Hence, the effective area of the receiver is also affected by any angular misalignment between the source and the receiver. The reduction in signal in dB due to beam spreading may be approximated by:

$$L_{spread} = 20log_{10} \left[ \frac{D\sqrt{\cos\gamma}}{2d\tan(\theta/2)} \right] dB, \quad (4)$$

where $d$ is the transducer separation and $\gamma$ is the angle of transducer misalignment as shown in Fig. 3. Note that with a small angle of misalignment, the effective reception area of the receiver is an ellipse rather than a circle. The influence of this type of alignment may be trivial in terms of signal strength, however, it may introduce phase distortion especially for phase modulation schemes. Since the ultrasonic field radiated by a transducer is not uniform in all directions, the directionality of the transducer has to be taken into account when the transceivers are not aligned in parallel. The ultrasonic radiation field in front of a transducer can be calculated using an impulse response method [22], [23]. The mathematical model assumes that the pressure at the observation point $M$ can be computed from the interference of the plane wave from the source, and edge waves which are diffracted at the boundaries of the source [24], [25]. The pressure impulse response $p(M,t)$ for an arbitrary point $M$ is defined as the differential of the velocity potential impulse response as follows:
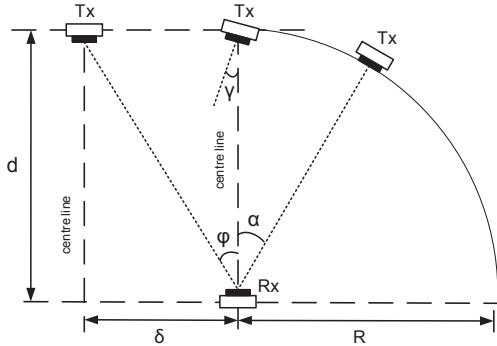
$$p(M,t) = \rho_0(\delta\Phi/\delta t)(M,t), \quad (5)$$

Fig. 3: Diagram of transducer arrangements with lateral displacement $\delta$, oblique angle $\alpha$, and small misalignment angle $\gamma$.



Fig. 4: Comparison of simulated response for attenuation, simplified beam spread, pressure field at 3 m.

where $\rho_0$ is the density of the medium. Recent work [26] recorded experimental results when different off-axis transducer displacements occurred that gave a reasonable match with the theoretical model for an ultrasonic communication channel at relatively short ranges. Fig. 4 compares the on-axis responses at 3 m using both the simplified beam spread model (4) and the full pressure field model (5), including their combined responses with the effects of attenuation. As can be seen, the simplified model shows that there should be less beam spreading at higher frequencies while the pressure field model gives almost a constant response at all frequencies. As a result, their combined responses after adding attenuation produced two different response curves which may affect the simulations significantly. The two models are compared with experimental results in the next section.

In addition to ultrasonic absorption and beam spreading, the system response measured over an air gap of 50 mm was also included in the simulation model. Note that 50 mm is the minimum separation of the transducers that can distinguish the original impulse signal from its reflected echoes from the surface of the transmitter. This system frequency response can then represent the transducer response over different frequencies without taking diffraction and absorption losses into account. The background noise in the air channel was adequately represented by additive white Guassian noise (AWGN), and was added to simulate electronic noise to match the experimental conditions more closely.

### B. Transmission and demodulation process

The diagram of a multi-channel OOK and BPSK modulator used to generate a suitable transmission digital waveform is shown in Fig. 5. The binary stream to be transmitted was sent into a bit splitter before distributing to 6 parallel channels. The split binary data were then encoded using a unipolar encoder and a non-return-zero encoder for OOK and BPSK schemes respectively. For OOK, the voltage level used for a bit "1" was +1 V and a bit "0" was 0 V. For BPSK, a bit "1" was equal to +1 V and a bit "0" was equal to -1 V to provide a 180°phase change before being modulated to different carrier waves. The 6 message sequences $m_1(t)$ to $m_6(t)$ were then filtered by a raised cosine filter before simultaneously modulating to carrier frequencies from 50 kHz to 110 kHz at 12 kHz
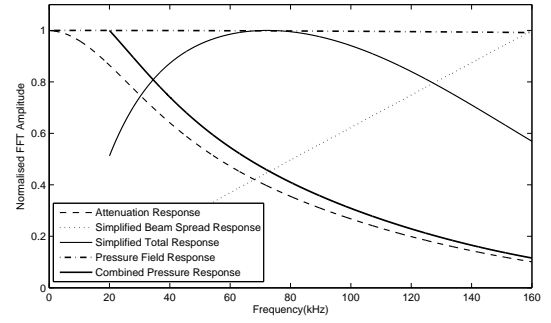
channel spacing. All these modulated signals were finally added together, giving a single waveform $S(t)$. Before the data signal was finally downloaded to the waveform generator, a windowed sinc-like synchronization signal containing frequency components in all 6 channels with a duration of 0.03 ms was added to the front of the information signal for ultrasonic triggering of the oscilloscope. This was to generate a resistant signal with rapid and transient changes in amplitude using all 6 primary transmission channel frequencies which was not overwhelmed by background noise especially at long transmission ranges. This completely removed the need for a hard-wired trigger as used in previous studies by other authors. The trigger impulse had an amplitude larger than the amplitude of the information signal so that the oscilloscope could reliably trigger from a higher amplitude signal as the amplitudes of the data signal varied.

A typical multi-channel OOK and BPSK demodulator is shown in Fig. 6. The received six-channel signal $S_n(t)$ was band-pass filtered by a Butterworth filter to extract the different frequency channels. Phase shift was minimised by implementing a zero-phase filter which processed the input data in both forward and reverse directions. For multi-channel OOK, the filtered signals at individual channels were envelope detected using a Hilbert transform [27] before being decoded by bit comparators. For BPSK demodulation, the filtered signal was multiplied by a coherent reference carrier with the corresponding frequency in that channel. The resultant waveform was low-pass filtered before being sent to a bit judge. All decoded bits were then combined into a single bit sequence. Demodulation processes for both OOK and BPSK schemes will be illustrated in Section V in more detail.
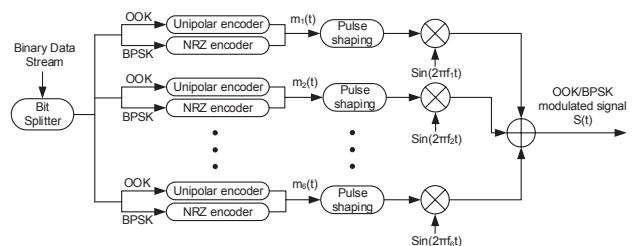


Fig. 5: Schematic diagram of the multi-channel on-off keying (OOK) and binary shift keying (BPSK) modulator.
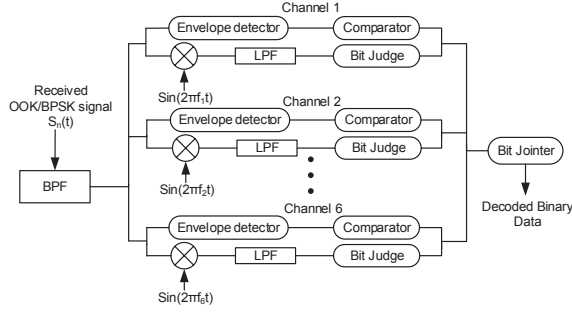
Fig. 6: Schematic diagram of the multi-channel on-off keying (OOK) and binary shift keying (BPSK) demodulator.



Fig. 8: Simulated OOK demodulation process over 3 m: (a) band-pass filtered OOK signal for letter 'e', (b) envelope of the filtered signal, (c) normalised energy bar plot under the curve of each bit duration. Experimental OOK demodulation process: (d) band-pass filtered OOK signal for letter 'e', (e) envelope of the filtered signal, (f) normalised energy bar plot under the curve of each bit duration.

## V. RESULTS AND DISCUSSION

### A. Preliminary experiments

All experiments were carried out in an indoor laboratory with negligible air turbulence and a low multi-path interference set-up. Room temperature was measured at $20°C$ under an atmospheric pressure of approximately 1 atm, and the relative humidity recorded was around 72%. Transmitter and receiver transducers were laser aligned to have coincident center normals, allowing ease of simulation. Example characters "Hello!" were encoded and modulated using the OOK modulation scheme described previously. Each character was represented by 8 bits with a bit duration of 0.1 ms. Since there were 6 channels transmitted simultaneously, the system data rate achieved was 60 kb/s. Fig. 7 illustrates simulated received OOK signals using both simplified and pressure field models compared to the experimental signal in the time and frequency domains over 3 m, respectively. As can be seen, all three time domain signals in Fig. 7 (a), (c) and (e) are visually similar. In the frequency domain, good agreement between the simulated signal using the simplified beam spread model and the actual experimental signal can be seen in Fig. 7 (d) and (f). However, the simulated signal spectra using the full pressure field model in Fig. 7 (b) gives a steeper decay along the frequency axis

which does not match the experiment well. Therefore, to predict different frequency signals more accurately and also to save computational effort, the simplified model was used instead of the full pressure field model for on-axis transducer set-ups. Note that only OOK signals and spectra are presented here as illustrative examples; similar good agreement was achieved with BPSK.

The demodulation process of both simulation and experiment for OOK signals over 3 m is illustrated in Fig. 8. The simulated filtered signal in Fig. 8 (a) represents the second character 'e' as an illustrative example. As can be seen, amplitude peaks can be clearly identified to distinguish logic "1"s and "0"s. Fig. 8 (b) presents the plotted envelope by taking its absolute value. Afterwards, the energy under the curve over the central 20% of each bit period was calculated and normalised, giving the bar plot shown in Fig. 8 (c). This is to minimise the energy leakage effects so that the differences between energies of "1"s and "0"s are sufficiently distinct to deliver correct decoding results when compared with a threshold value. The threshold value was determined by a large number of error tests over short, medium and long ranges. 12000 packets of six 8-bit random ASCII code sequences were modulated and simulated over distances of 0.2 m, 2 m and 5 m with SNR values of 3 dB, 25 dB and 35 dB respectively. Numbers of errors were collected in terms of different energy threshold values from 0 to 1 with a step of 0.01. The minimal numbers of errors all occurred when using a threshold value of 0.28 over the three different distances.
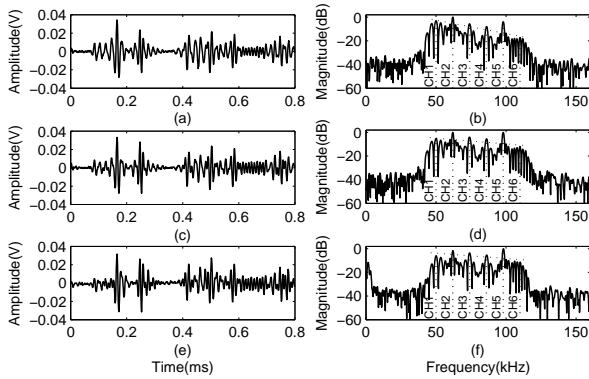


Fig. 7: Comparison of simulated and experimental signals over 3 m: (a) time domain simulated received OOK signal using pressure field model, (b) its spectra, (c) time domain simulated received OOK signal using simplified model, (d) its spectra, (e) time domain received OOK signal and (f) its spectra. Note that CH1 - CH6 are channel 1 to channel 6. The frequency trend is indicated in (b), (d) and (f) by a dotted line.
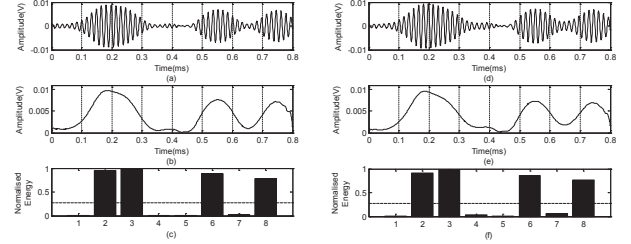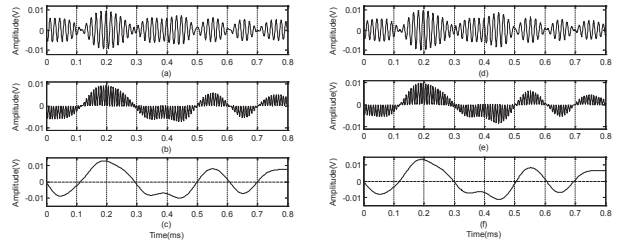


Fig. 9: Simulated BPSK demodulation process over 3 m: (a) band-pass filtered BPSK signal for letter 'e', (b) waveform after coherent multiplication, (c) low-pass filtered signal of the waveform in (b). Experimental BPSK demodulation process: (d) band-pass filtered OOK signal for letter 'e', (e) waveform after coherent multiplication, (f) low-pass filtered signal of the waveform in (e).
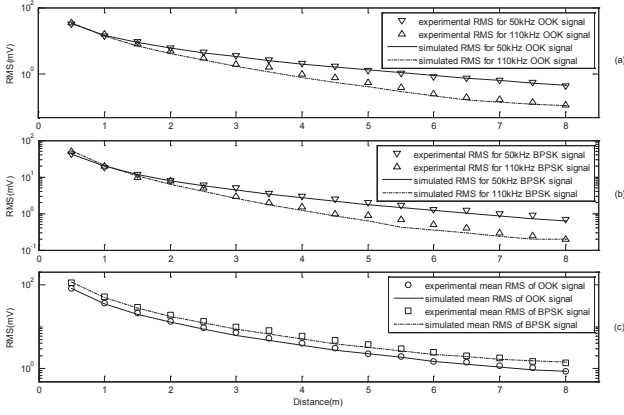
Fig. 10: Comparison of experimental signal RMS values with theoretical predictions over different distances for: (a) 50 kHz and 110 kHz OOK signals, (b) 50 kHz and 110 kHz BPSK signals and (c) combined 6-channel OOK and BPSK signals.
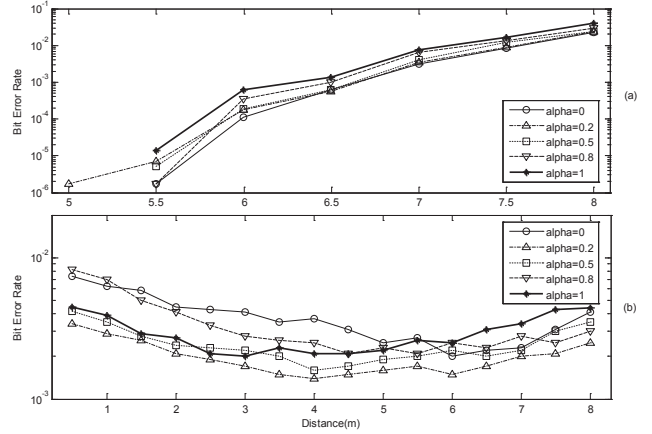


Fig. 11: Comparison of the experimental BER for both (a) OOK and (b) BPSK signals over different transmission distances using different roll-off factors.

Therefore, the demodulation threshold value was set at 0.28. Accordingly, the experimental demodulation in Fig. 8 (d), (e) and (f) show a good match with the simulation. Simulated and experimental demodulations of the BPSK scheme described previously are also compared in Fig. 9. The figures show a good prediction by the simulation. Fig. 9 (b) shows the simulated result after the coherent multiplication of the band-pass filtered signal in Fig. 9 (a). If the amplitude of the low-pass filtered signal in Fig. 9 (c) detected at the centre of each bit duration was larger than 0, a bit "1" is extracted; conversely, an amplitude smaller than 0 implies a bit "0" was decoded. As can be seen in the experimental demodulation in Fig. 9 (e) and (f), the opposite phases for "1"s and "0"s are clearly displayed after coherent multiplication and it is straightforward to decode the low-pass filtered signals.

Over propagation distances ranging from 0.5 m to 8 m with a step of 0.5 m, the RMS values of both the experimental OOK and BPSK signals at different frequencies can be accurately predicted by the theory as Fig. 10 (a) and Fig. 10 (b) show. The figures again illustrate that the low frequency signals have smaller RMS values over short ranges than high frequency signals for both OOK and BPSK modulation schemes due to beam spreading. However, at longer propagation ranges, atmospheric absorption starts to increase and become dominant. The mean RMS curve for the combined signal of all six channels over different ranges is simulated in Fig. 10 (c). It should be noted that as a constant-envelope modulation, BPSK scheme produces signals with higher RMS values over all ranges than OOK signals. It also indicates that the model in this work can be used to simulate other modulation schemes and predict signals as the simulated curves match the experimental data well.

### B. Bit error rate analysis

To further investigate the reliability of the system, it was necessary to look at the bit error rate (BER) of both modulation schemes over different ranges. Therefore, 1200 packets of six 8-bit random binary ASCII code streams were generated and transmitted continuously through the channel. BER informa-

tion was recorded over transducer separations of up to 8 m at increments of 0.5 m. The process was repeated 10 times, and the results were then averaged. The BER results for OOK and BPSK schemes using different roll-off factors are illustrated in Fig. 11 (a) and Fig. 11 (b) respectively. As can be seen in Fig. 11 (a), the OOK scheme started to have decoding errors at 5 m using different roll-off factors from 0 to 1. The BER increases with the transmission distance for all roll-off factors after that. It is obvious that with a zero roll-off the errors were at the lowest level at all distances, and it gave the system error-free transmission up to 5.5 m. However, in Fig. 11 (b), the BER for the BPSK scheme drops from a high level at short distances before rising up again after 5 m. It is been proved that most of the errors occurring at short ranges are due to the echo signal reflected from the surface of the transmitter, as the number of errors drops significantly when the receiver is placed with an oblique angle to the transmitter centreline. It is noticed that the number of errors using the BPSK scheme over long ranges is much smaller than that using the OOK scheme. Again, a roll-off factor of 0.2 which provides the lowest BER for the BPSK scheme can be determined from this figure. It is intuitive to visualize the signal distortion using eye diagrams as shown in Fig. 12. As can be seen, over 3 m, both the 50 kHz and 110 kHz OOK signals have more open eyes in Fig. 12 (a)
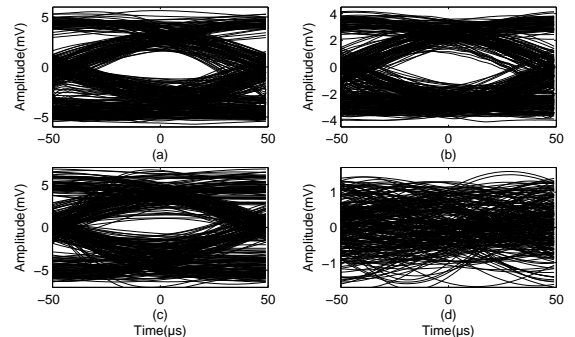


Fig. 12: Eye diagrams for OOK signals in 50 kHz (a) and 110 kHz (b) channels and BPSK signals in 50 kHz (c) and 110 kHz (d) channels over 3 m.

and (b) than those of the BPSK signals in Fig. 12 (c) and (d). Therefore, it indicates that the OOK signals in both low and high frequency channels are less distorted than the BPSK signals. The eye of the 110 kHz BPSK signal in Fig. 12 (d) is completely closed. Note that narrow-band transducers have a relatively high-Q resonant response so that there is insufficient channel spacing to accurately represent fast phase changes, especially for high frequency BPSK signals in a multi-channel scheme.

Previous work on multi-channel communication investigated high frequency ASK at 250 kHz with only a 0.5 m transmission distance and achieved an 80 kb/s data transfer rate using prototype transducers [28]. The spectral efficiency of the system measured in b/s/Hz was 0.76. However, in this work, the over-all system data rate achieved was up to 60 kb/s using a pair of commercially available SensComp 600 ultrasonic transducers. The bandwidth efficiency was 1 b/s/Hz, which is 32% higher compared to the previous work. System performance was tested in terms of the BER characteristics. The BER results shows that the OOK modulation scheme implemented here was capable of achieving error free decoding over ranges of up to 5 m. Previous short-range work by other authors [8] suffered from much higher BER (50% at 2.38 m) at a data rate of 83 kb/s using a single-band OOK modulation scheme, with error-free transmission only at ranges below 1.6 m.

## VI. RANGE-DEPENDENT MODULATION SCHEME

In order to have more effective transmission, a multi-channel scheme is proposed using different modulation schemes depending on the range to ensure error-free transmission. Over short ranges, data rates for different channels can be slightly increased using reduced bit times and different channel spacings. The channel arrangement detail is shown in Table I. As can be seen, only five channels were used, and all of them were sampled at an integer number of cycles during each bit period. This prevents signal discontinuities, thus reducing unnecessary spectral leakage. The lowest frequency channel (Channel 1) and highest frequency channel (Channel 5), which most suffered from beam spreading loss and ultrasonic absorption respectively, contributed slightly lower data rates than the medium frequency channels so that they had relatively longer bit durations. The total system data rate achieved using this channel arrangement was 63 kb/s. It is 5% higher than the data rate achieved by using the previous fixed-bit-duration and fixed-channel-spacing multichannel OOK modulation scheme with six channels. This scheme experienced error-free decoding over ranges up to 2 m. For long range ultrasonic transmission, the most distorted channels (50 kHz channel and 110 kHz channel) were not used and a larger channel spacing was assigned between medium frequency channels as shown in Table II. The data rate achieved was half of the original OOK scheme. However, this new scheme only started to experience transmission errors beyond 7.5 m. As Fig. 11 (b) indicates, much less error occurs when using a multi-channel BPSK scheme than when using a multi-channel OOK scheme over long ranges. Therefore, it is possible to re-use BPSK modulation over longer ranges with a reduced data rate. The

TABLE I: Channel arrangement over error-free ranges up to 2 m

|  | CH1 | CH2 | CH3 | CH4 | CH5 |
|---|---|---|---|---|---|
| Operating frequency (kHz) | 50 | 63 | 78 | 94 | 110 |
| Number of cycles | 5 | 5 | 5 | 7 | 10 |
| Data rate (kb/s) | 10 | 12.6 | 15.6 | 13.4 | 11 |

TABLE II: Channel arrangement over error-free ranges up to 10 m

|  | CH1 | CH2 | CH3 |
|---|---|---|---|
| Operating frequency (kHz) | 60 | 80 | 100 |
| Number of cycles | 6 | 8 | 10 |
| Data rate (kb/s) | 10 | 10 | 10 |

same channel allocation in Table II was implemented using BPSK modulation, and the error-free range was extended to 10 m according to the experimental results. The eye diagrams of 3-channel OOK and BPSK signals over 8 m are compared in Fig. 13. As can be seen, BPSK signals have better eye shapes with less jitter and amplitude variation in all three channels than OOK signals. The BER results of different schemes can be used as an indicative guide in a two-way communication system when distance measurement is available. Within 2 m, 5-channel OOK with a data rate of 63 kb/s could be used. Between 2 and 5 m, the system switched to 6-channel OOK with 60 kb/s data transfer rate. Beyond 5 m, the error-free transmission range could be achieved using 3-channel BPSK modulation scheme with a reduce data rate of 30 kb/s. The transmission distance can be estimated based on the received signal strength (RSS) [29], [30]. As the RMS values of the received signal in different propagation ranges can be predicted by the simulation model, different schemes are chosen in terms of the distance measured. Token signals according to the scheme used should be added and sent with the output signal to initialize the corresponding demodulation scheme. Therefore, a reliable two-way indoor ultrasonic link up to 10 m should be possible using the range-dependent scheme.

## VII. TRANSDUCER MISALIGNMENT

The situation when the transducer centre normals are not coincident over long ranges was also studied in this work. As Fig. 3 shows, the receiver transducer (Rx) was placed away from the transmitter transducer (Tx) at a distance $d = 5$ m. The maximum distance of lateral displacement for error-free
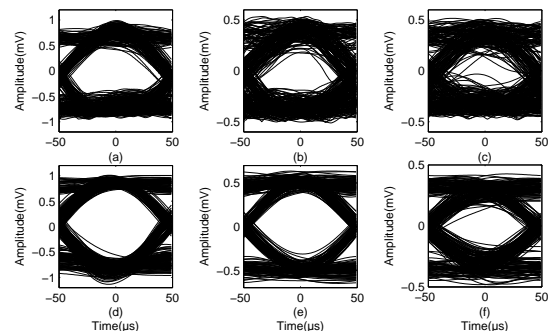


Fig. 13: Eye diagrams for OOK signals in 60 kHz (a), 80 kHz (b) and 100 kHz (c) channels and BPSK signals in 60 kHz (d), 80 kHz (e) and 100 kHz (f) channels over 8 m.

TABLE III: Comparison of BER using OOK and BPSK schemes at
0.4 m lateral displacement

| BER | Over-all | CH1 | CH2 | CH3 |
|---|---|---|---|---|
| OOK | 1.79e-2 | 0 | 1.18e-4 | 1.78e-2 |
| BPSK | 1.17e-3 | 0 | 0 | 1.17e-3 |

TABLE IV: Comparison of BER using OOK and BPSK schemes at
$7°$ oblique angle

| BER | Over-all | CH1 | CH2 | CH3 |
|---|---|---|---|---|
| OOK | 8.12e-3 | 0 | 0 | 8.12e-3 |
| BPSK | 9.43e-4 | 0 | 0 | 9.43e-4 |



Fig. 14: Comparison of experimental signal RMS values with theoretical predictions with different: (a) lateral displacements and (b) oblique angles at a transducer separation of 5 m.

transmission using the 3-channel scheme illustrated in Table II for both OOK and BPSK modulation was found to be 0.35 m, i.e. $\delta = 0.35$ m or 7% of '$d$'. At this distance, the transducers were separated at an angle $\varphi = 4°$. The beam spreading angle for the highest frequency channel (100 kHz channel) is $6.3°$, and for the lowest frequency channel (60 kHz channel) is $10.5°$. In this case, all frequency channel signals can still be detected by the receiver transducer. As Table III shows, the 3-channel BPSK scheme has a much better performance than the 3-channel OOK scheme at 0.4 m lateral displacement in terms of the BER results over all channels. The BER reduces with decreasing channel frequency for both schemes as expected, as less high frequency energy can reach the receiver transducer. Apart from the lateral displacement experiment, it is also interesting to study the bit error tolerance when the two transducers are placed with different oblique angles as also shown in Fig. 3. The transmitter was separated from the receiver by a radius of $R = 5$ m, and the BER tests were carried using different oblique angles $\alpha$ with $1°$ increment. The results show that the bit errors started to occur at an oblique angle of $7°$ for both 3-channel OOK and BPSK schemes. Bit error details are shown in Table IV. As can be seen, the high frequency channels are more prone to error, and the BPSK scheme is more robust than the OOK scheme in terms of BER characteristics. Fig. 14 (a) and (b) compare the signal RMS values with theoretical predictions using the full pressure field model with different lateral displacements and oblique angles respectively, and good agreements were found between the two. From both lateral displacement and oblique angle experiments, it suggests that alignment for ultrasonic communication is important though the system can tolerate errors with a small amount of lateral displacement and oblique angles. Thus, divergent or omnidirectional transducers are required. It also shows that low frequency signals are a better choice than high frequency signals for error-free transmission with misaligned transducers.

## VIII. CONCLUSIONS AND FUTURE WORK

It has been shown, in both simulation and experiment, that multi-channel error-free data communication using both OOK and BPSK modulation schemes was practical over ranges up to 10 m. By using a pair of commercially available ultrasonic transducers with a nominal frequency of 50 kHz, all results were based on multi-channel transmission operating within frequencies from 50 kHz to 110 kHz in terms of 6 dB bandwidth. The maximum data rate achieved using a single
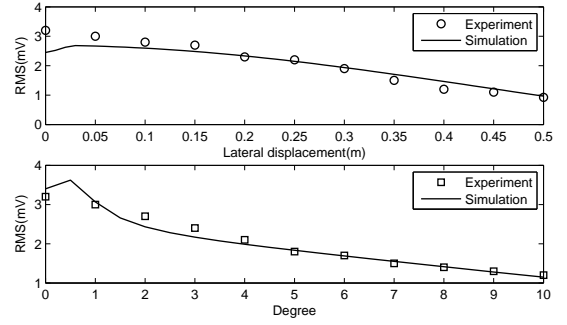
modulation scheme was 60 kb/s, with 6 parallel 8-bit channels being represented by 0.8 ms duration time signals. System bandwidth efficiency was 100% in b/s/Hz. Ultrasonic signals were simulated including the effects of ultrasonic absorption in air, beam spreading loss, transducer response and AWGN. Simulation predicted the signals successfully, and had an excellent agreement with the experimental results based on signal characteristics in both time and frequency domains, the demodulation process and RMS values over different transmission ranges. BER performance was characterised over different distances, and error-free decoding was achieved at ranges of up to 5 m using a multi-channel OOK scheme. More reliable long-range links were also achieved by using a range-dependent multi-channel modulation scheme. Individual bit times were assigned to each channel to achieve error-free transmission over all ranges up to 10 m using a combination of OOK and BPSK schemes. Transducer arrangements with lateral displacements and oblique angles were tested using both multi-channel OOK and BPSK giving error-free transmission at reduced data rates. It was concluded that 3-channel BPSK was more robust than 3-channel OOK in both aligned and misaligned conditions. Wireless synchronization was also achieved by ultrasonic means, instead of by hard-wired link as used in previous works. This study focuses on LOS simplex communication. However, in practice, a duplex system is desirable, as the system could then easily detect the transmission range and apply a self-adaptive range-dependent modulation scheme, which is currently under investigation. There are many potential applications for the system, including a secure network in an indoor office environment. Each device may have individual access sharing the same operating band without interfering with each other. Alternatively, ultrasonic base stations may be installed on the ceiling of a room to allow mobile access using an ultrasonic handover technique between base stations. Non-LOS conditions occur regularly in an indoor environment and the effects of reflection, diffraction and multipath interference will be considered in future studies.

## REFERENCES

[1] R. Kraemer and M. Katz, *Short-Range Wireless Communications: Emerging Technologies and Applications*, ser. WILEY-WWRF SERIES. Wiley, 2009.
[2] R. Ramirez-Iniguez, S. Idrus, and Z. Sun, *Optical Wireless Communications: IR for Wireless Connectivity*. Taylor & Francis, 2008.

[3] N. Borisov, I. Goldberg, and D. Wagner, "Intercepting mobile communications: the insecurity of 802.11," in *Proceedings of the 7th annual international conference on Mobile computing and networking*, ser. MobiCom '01. New York, NY, USA: ACM, 2001, pp. 180–189.

[4] W. Manthey, N. Kroemer, and V. Magori, "Ultrasonic transducers and transducer arrays for applications in air," *Meas. Sci. Technol.*, vol. 3, pp. 249–261, 1992.

[5] R. A. Zurek, A. Dietrich, and M. L. Charlier, "Omnidirectional ultrasonic communication system," U.S. Patent 6 363 139, Mar. 26, 2002.

[6] L. Hofmann, "Transmission of data by ultrasound," U.S. Patent 6 950 681, Sep. 27, 2005.

[7] S. Holm, O. Hovind, S. Rostad, and R. Holm, "Indoors data communications using airborne ultrasound," in *Acoustics, Speech, and Signal Processing, 2005. Proceedings. (ICASSP '05). IEEE International Conference on*, vol. 3, 2005, pp. 957–960.

[8] C. Li, D. Hutchins, and R. Green, "Short-range ultrasonic digital communications in air," *Ultrasonics, Ferroelectrics and Frequency Control, IEEE Transactions on*, vol. 55, no. 4, pp. 908–918, 2008.

[9] ——, "Short-range ultrasonic communications in air using quadrature modulation," *Ultrasonics, Ferroelectrics and Frequency Control, IEEE Transactions on*, vol. 56, no. 10, pp. 2060–2072, 2009.

[10] W. Jiang and W. M. D. Wright, "Wireless communication using ultrasound in air with parallel OOK channels," in *Signals and Systems Conference (ISSC 2013), 24th IET Irish*, June 2013, pp. 1–6.

[11] A. Ens, T. Janson, L. M. Reindl, and C. Schindelhauer, "Robust multicarrier frame synchronization for localization systems with ultrasound," in *OFDM 2014; 18th International OFDM Workshop 2014 (InOWo'14); Proceedings of*, Aug 2014, pp. 1–8.

[12] T. Hosman, M. Yeary, and J. K. Antonio, "Design and characterization of an mfsk-based transmitter/receiver for ultrasonic communication through metallic structures," *Instrumentation and Measurement, IEEE Transactions on*, vol. 60, no. 12, pp. 3767–3774, Dec 2011.

[13] J. Proakis and M. Salehi, *Digital Communications*. McGraw-Hill Higher Education, 2008.

[14] E. McCune, *Practical digital wireless signals*. Cambridge University Press, 2010.

[15] W. Jiang and W. M. D. Wright, "Multi-channel indoor wireless data communication using high-k capacitive ultrasonic transducers in air," in *Ultrasonics Symposium (IUS), 2013 IEEE International*, July 2013, pp. 1606–1609.

[16] K. Pahlavan and A. Levesque, *Wireless Information Networks*. Wiley, 2005.

[17] (2015, Aug.) The senscomp website. [Online]. Available: http://www.senscomp.com/pdfs/series-600-environmental-grade-sensor.pdf

[18] W. Mason and R. Thurston, Eds., *Physical acoustics: principles and methods*, ser. Physical Acoustics. Academic Press, 1984.

[19] H. E. Bass, L. C. Sutherland, A. J. Zuckerwar, D. T. Blackstock, and D. M. Hester, "Atmospheric absorption of sound: Further developments," *The Journal of the Acoustical Society of America*, vol. 97, no. 1, pp. 680–683, 1995.

[20] J. Krautkrämer and H. Krautkrämer, *Ultrasonic testing of materials*. Springer-Verlag, 1990.

[21] R. Halmshaw, *Non-destructive testing*. Edward Arnold, 1987.

[22] P. R. Stepanishen, "Transient radiation from pistons in an infinite planar baffle," *The Journal of the Acoustical Society of America*, vol. 49, no. 5B, pp. 1629–1638, 1971.

[23] J. C. Lockwood and J. G. Willette, "High-speed method for computing the exact solution for the pressure variations in the nearfield of a baffled piston," *The Journal of the Acoustical Society of America*, vol. 53, no. 3, pp. 735–741, 1973.

[24] A. G. Bashford, D. W. Schindel, D. A. Hutchins, and W. M. D. Wright, "Field characterization of an air-coupled micromachined ultrasonic capacitance transducer," *The Journal of the Acoustical Society of America*, vol. 101, no. 1, pp. 315–322, 1997.

[25] D. A. Hutchins, J. S. McIntosh, A. Neild, D. R. Billson, and R. A. Noble, "Radiated fields of capacitive micromachined ultrasonic transducers in air," *The Journal of the Acoustical Society of America*, vol. 114, no. 3, pp. 1435–1449, 2003.

[26] C. Li, D. Hutchins, and R. Green, "Response of an ultrasonic communication channel in air," *Communications, IET*, vol. 6, no. 3, pp. 335–343, February 2012.

[27] Y. Shmaliy, *Continuous-time signals*. Springer, 2006.

[28] W. M. D. Wright, O. Doyle, and C. T. Foley, "Multi-channel data transfer using air-coupled capacitive ultrasonic transducers," in *Ultrasonics Symposium, 2006. IEEE*, 2006, pp. 1805–1808.

[29] S. Holm, "Ultrasound positioning based on time-of-flight and signal strength," in *Indoor Positioning and Indoor Navigation (IPIN), 2012 International Conference on*, Nov 2012, pp. 1–6.

[30] C. Medina, J. Segura, and S. Holm, "Feasibility of ultrasound positioning based on signal strength," in *Indoor Positioning and Indoor Navigation (IPIN), 2012 International Conference on*, Nov 2012, pp. 1–9.
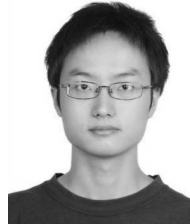
**Wentao Jiang** received the B.Eng. in Communications Engineering from Zhejiang University of Technology, China, in 2010. He then continued his study and received the M.Sc. in Communications Engineering from University of York, England, in 2012. He is currently doing full-time Ph.D. research in air-coupled ultrasonic communication at University College Cork, Ireland. His research interests are in capacitive ultrasonic transducers, digital modulation and signal processing.

**William M.D. Wright** received his BEng and PhD degrees in mechanical engineering from the University of Warwick, England in 1991 and 1996, respectively. He continued to work there as a post-doctoral researcher until 1997, when he joined the School of Engineering in University College Cork, Ireland where he is currently Senior Lecturer in Mechanical Engineering. His research interests include non-contact ultrasonic measurements, design and development of capacitive ultrasonic transducers, ultrasonic flow metering in gases, and ultrasonic communications. He is a member of the Acoustical Society of America, a Senior Member of the IEEE and an Associate Editor of IEEE Trans. UFFC.